Free Radical Biology and Medicine 134 (2019) 545–554

Contents lists available at ScienceDirect

Free Radical Biology and Medicine

journal homepage: www.elsevier.com/locate/freeradbiomed

Short communication

New red-shifted fluorescent biosensor for monitoring intracellular redox changes

Claudia Vanesa Piattoni[a,1], Florencia Sardi[b,1], Florencia Klein[c], Sergio Pantano[c], Mariela Bollati-Fogolin[a], Marcelo Comini[b,*]

[a] Cell Biology Unit, Institut Pasteur de Montevideo, Mataojo 2020, CP 11400, Montevideo, Uruguay
[b] Laboratory Redox Biology of Trypanosomes, Institut Pasteur de Montevideo, Mataojo 2020, CP 11400, Montevideo, Uruguay
[c] BioMolecular Simulation Group, Institut Pasteur de Montevideo, Mataojo 2020, CP 11400, Montevideo, Uruguay

ARTICLE INFO

Keywords:
Glutathione
Oxidation
Thiol
Molecular simulation
Ruby
Clover

ABSTRACT

Maintenance of intracellular redox homeostasis is critical for cell survival, proliferation, differentiation, and signaling. In this regard, major changes in the intracellular redox milieu may lead to cell death whereas subtle increases in the level of certain oxidizing species may act as signals that regulate a plethora of cellular processes. Redox-sensitive variants of green fluorescent proteins (roGFP2 and rxYFP) were developed and proved useful to monitor intracellular redox changes in a non-invasive and online manner. With the aim to extend the spectral range of the fluorescent redox biosensors, we here describe the generation, biochemical characterization and biological validation of a new redox reporter based on the red-shifted mRuby2 protein (rxmRuby2). Spectrofluorimetric analysis performed with the recombinant biosensor shows a reversible redox response produced by two redox-active cysteine residues predicted by molecular modeling. rxmRuby2 is highly selective for the couple glutathione/glutathione disulfide in the presence of the oxidoreductase glutaredoxin. The estimated redox potential of rxmRuby2 (E° -265 ± 22 mV) makes it suitable for its use in reducing subcellular compartments. Titration assays demonstrated the capacity of rxmRuby2 to monitor redox changes within a physiological pH range. rxmRuby2 responded sensitively and reversibly to different redox stimuli applied to HeLa and HEK293 cells expressing transiently and/or stable the biosensor. Fusing rxmRuby2 to the Clover fluorescent protein allowed normalization of the redox signal to the expression level of the reporter protein and/or to other factors that may affect fluorescence. The new red-shifted redox biosensor show promises for deep-tissue and *in vivo* imaging applications.

1. Introduction

Several processes such as growth, differentiation, signaling, and death are, to some extent, modulated by the redox state of the cell. In most living organisms, the thioredoxin and the glutaredoxin systems act concertedly to maintain the thiol-disulfide redox homeostasis and regulate protein function [1,2]. These systems are not in equilibrium between each other neither display a homogeneous distribution within the different subcellular compartments and domains [3–6]. Thus, the assessment of the redox state of cells requires the development of sensors that do not perturb cell physiology and are capable to report the dynamics of the redox changes in a sensitive and specific manner (e.g. compartment, redox system). Most of these requirements are met by genetically encodable biosensors consisting of redox-sensitive fluorescent proteins (rsFP) [7–10].

Conversion of a fluorescent protein into a redox biosensor can be achieved by including a surface-exposed cysteine pair with capacity to form an intramolecular disulfide bridge that, by allosterism, may influence the spectral properties of the chromophore [11,12]. Several redox-sensitive variants of the green fluorescent protein were generated using this approach [7–10 and references therein]. In biological systems, the rsFP showed selectivity for detecting changes in the ratio

Abbreviations: $E^{0'}$, midpoint redox potential; *E. coli*, *Escherichia coli*; FI, fluorescence intensity; FBS, fetal bovine serum; FP, fluorescent protein(s); Grx, glutaredoxin; GSH, reduced glutathione; GSSG, oxidized glutathione; H_2O_2, hydrogen peroxide; RF, restriction free; roGFP2, redox sensitive green fluorescent protein; rsFP, redox sensitive fluorescent proteins; rxRFP, redox sensitive red fluorescence protein; rxmRuby2, redox sensitive mRuby2 fluorescent protein; rxYFP, redox sensitive yellow fluorescent protein; WT, wild type

* Corresponding author.
E-mail address: mcomini@pasteur.edu.uy (M. Comini).
[1] Both authors contributed equally to this work.

https://doi.org/10.1016/j.freeradbiomed.2019.01.035
Received 14 September 2018; Received in revised form 24 January 2019; Accepted 24 January 2019
Available online 05 February 2019
0891-5849/

glutathione/glutathione disulfide (GSH/GSSG) and rapid equilibration kinetics mediated by the thiol-disulfide oxidoreductase glutaredoxin (Grx) [6,10,12–14].

Recently, circularly permuted redox-sensitive red fluorescent proteins (rxRFP with λex/λem 576/600 nm) embracing different redox potentials have been generated [15,16]. Disulfide bond formation between the cysteines located at the N- and C-termini of rxRFP stabilizes the chromophore leading to a 4-fold increase in fluorescence at physiological pH [15]. A major drawback of this biosensor is that under reducing conditions the chromophore remains accessible to the solvent and thus prone to be quenched by protonation (pH < 8) and/or to be oxidized by ONOOH and $O_2^{\bullet-}$ [15]. Thus, quantitative measurements with rxRFP require the analysis of the parental cell line expressing a redox-insensitive RFP to subtract the influence of proton concentration or direct oxidative modification of the chromophore.

Here we present the rational design, biochemical and biological characterization of a novel red-shifted redox biosensor based on the mRuby2 fluorescent protein [17].

2. Materials and methods

2.1. Reagents

Unless otherwise indicated, all chemicals used were of the highest grade and purchased from Sigma Aldrich. Media, fetal bovine serum (FBS) and consumables for cell culture were obtained from Thermo Fisher Scientific, Invitrogen, PAA, and Greiner.

2.2. Molecular design of redox biosensor

Structural superposition of protein coordinates was performed with STAMP [18] as implemented in VMD [19]. Molecular models of mRuby2 and 3 were performed using Modeller 9.17 [20] and the available atomic coordinates of mRuby1 as the template (PDBid: 3U0N). Electrostatic profiles were calculated with APBS 1.0 [21]. To reduce the dependence of the electrostatic potential profiles upon side chain rotamers, the calculations were performed on coarse-grained structures according to the simplified representation proposed in Ref. [22].

2.3. Expression vectors

The pCDNA3.1/Clover-mRuby2 vector, suitable for expression of the wild-type form (WT) of the fluorescent proteins in mammalian cells, was purchased from Addgene. The redox-sensitive version of Clover-mRuby2, named Clover-rxmRuby2 or RXM (mutant C49T for Clover and C118S/T148C/D200C for mRuby2) was *de novo* synthesized and inserted into a pUC57 plasmid (Biobasic). The Clover-rxmRuby2 sequence was subcloned into the expression vectors pCDNA3.1 and pET-TRX1b by a restriction-free (RF) method using as template pUC57/Clover-rxmRuby2 and the oligonucleotides: Fwd 5′-GTAACGGCCGCCA GTGTGCTGGAATTCGGCATGGTCTCCAAGGGCGAGG-3′ and Rev 5′-CCGCCAGTGTGATGGATATCTGCAGAATTCTTATTTATACAGTTCGT CCATACC-3′. For the RF subcloning, two sequential PCR was performed in a total reaction volume of 50 µL. The first PCR reaction consisted of 10 ng of pUC57/Clover-rxmRuby2 plasmid, 0.5 µM of each primer, 0.2 mM dNTP, 1X GC buffer and 1 U Phusion® High-Fidelity DNA polymerase (New England BioLabs Inc). The PCR program consisted of 30 cycles at 95 °C for 10 s, 60 °C for 30 s and 72 °C for 150 s, and a final incubation at 72 °C for 10 min. The amplicons were purified from an agarose gel (1% w/v) with a Wizard SV gel & PCR Clean-Up system (Promega), according to the manufacturer's instructions, and used as megaprimers in the subsequent RF step. RF reactions were performed with 20 ng of target DNA plasmid, 100 ng of mega-primers, 0.2 mM dNTP, 1.5% DMSO, 1X GC buffer and 1 U Phusion® High-Fidelity DNA Polymerase. The program used for RF consisted of a single denaturation step (98 °C, 2 min) followed by 20 cycles at 98 °C for 30 s, 68 °C for 30 s and 72 °C for 8 min, and a final elongation step of 10 min at 72 °C. Upon completion of the RF reaction, the parental plasmid DNA was eliminated by DpnI treatment (20 U enzyme per 10 µl of the linear-amplification reaction) for 2 h at 37 °C. *Escherichia coli* (*E. coli*) TOP 10 F′ cells were then transformed with the DpnI-digested RF reaction. Sequence insertion and correctness was confirmed by DNA sequencing (Macrogen, Korea) of plasmids isolated from bacteria.

To generate the rxmRuby2 expression vectors, the target sequence was amplified by PCR from pCDNA3.1/Clover-rxmRuby2 using the primers: Fwd 5′-GGATCCTATGGTGAGCAAAGGTGAAGAACTGATC-3′ and Rev 5′-AAGCTTTTTATACAGTTCGTCCATACCACCGCC-3′. The PCR reaction (50 µL final volume) contained 10 ng of pUC57/Clover-rxmRuby2 plasmid, 1 µM of each primer, 0.2 mM dNTP, 1.5 mM Mg^{2+}, 1X Taq buffer and 1 U Taq DNA Polymerase (Invitrogen). The PCR program consisted of 30 cycles at 95 °C for 30 s, 55 °C for 30 s and 72 °C for 2 min, and a final extension at 72 °C for 10 min. The amplicon was purified from agarose gel as described above and cloned into the TOPO-TA cloning vector (Invitrogen). The rxmRuby2-coding sequence was excised from this vector by enzymatic restriction with *Bam*HI and *Hind*III or *Bam*HI and *Eco*RI enzymes and further ligated into pre-digested pET22b (Novagen) or pCDNA3.1 (+) (Invitrogen) vectors, respectively, using standard protocols. The correctness of the cloned sequence was verified by sequencing both DNA strands (Macrogen, Korea).

2.4. Expression and purification of recombinant rxmRuby2

N-terminally His-tagged rxmRuby2 was expressed in *E. coli* strain BL21 (DE3) transformed with pET22b/rxmRuby2 and grown in LB medium supplemented with ampicillin 200 µg/mL. At an optical density (600 nm) of 0.8, IPTG (0.5 mM) was added to the culture and incubation resumed for 16 h at 25 °C. Cells were then harvested by centrifugation at 5,000 *g* for 20 min at 4 °C and the pellet resuspended in Buffer A (50 mM sodium phosphate pH 8.0, 300 mM NaCl) added of protease inhibitors (Protease inhibitor cocktail from Sigma-Aldrich and consisting of AEBSF, Bestatin, E−64, Pepstatin A, Phosphoramidon) and lysozyme (0.33 mg/mL). Cell lysis was completed by sonication on ice (three cycles at 45% power, 2 s pulse on/off, for 1 min) and debris was removed by centrifugation at 16,000 *g* for 1 h at 4 °C. His-tagged rxmRuby2 was purified by metal affinity chromatography in a 1 mL HisTrap column (GE Healthcare) pre-equilibrated with Buffer A. Protein elution was performed with a stepwise gradient from 0 to 500 mM imidazole. Elution fractions containing the protein of interest were pooled and concentrated by centrifugation (5,000 *g* at 4 °C) in a Vivaspin-20 filter (5 kDa cutoff). The concentrated protein sample was filtered through a 0.22 µm Millex GV filter (Millipore) and then injected (500 µL) onto a Superdex G75 10/300 GL column pre-equilibrated in PBS (pH 7.4) 1 mM EDTA. This gel filtration chromatography was performed at room temperature using an Äkta-FPLC system (Recombinant Protein Unit, Institut Pasteur de Montevideo), a flow rate of 0.8 mL/min and monitoring absorption at 280 nm and 560 nm. The purity of recombinant rxmRuby2 was of ~90% as judged by Coomassie-stained 15% SDS-PAGE (section ***3.2***).

2.5. Spectrofluorometric characterization of rxmRuby2

2.5.1. Redox assays

Fully reduced and oxidized rxmRuby2 wer prepared by incubating the protein (10 µM) with DTT (20 mM) or GSSG (2 or 5 mM) in PBS (pH 7.4) containing 1 mM EDTA for 1 h or 2 h, respectively, at room temperature. The excess low molecular weight reagents was removed by gel filtration on a Sephadex G25 (PD10 column, GE-Healthcare) equilibrated with PBS (pH 7.4) 1 mM EDTA. Protein concentration was measured at 280 nm (rxmRuby2 ε280 = 24.410 M^{-1} cm^{-1}) while the content of free-cysteine residues was estimated by reaction with 4,4′-

dithiodipyridine ($\varepsilon 324 = 21.400\ M^{-1}\ cm^{-1}$). The excitation ($\lambda_{ex}/\lambda_{em}$ 400–590/600 nm) and emission ($\lambda_{em}/\lambda_{ex}$ 580–700/560 nm) spectra of fully reduced and oxidized rxmRuby2 (5 μM) was recorded in a Cary Eclipse spectrofluorimeter using slit widths of 5 nm.

For the redox assays, a sample of fully reduced biosensor (5 μM) was incubated with 100 μM peroxynitrite (ONOOH), 250 μM hydrogen peroxide (H_2O_2), diamide, or glutathione disulfide (GSSG) with or without hGrx (5 μM), and fluorescence of rxmRuby2 (λex/λem = 560/600 nm) was recorded every 2 min in a Cary Eclipse spectrofluorimeter. Forty-six minutes later DTT (5 mM) was added to the samples and fluorescence was recorded for additional 46 min. In addition, rxmRuby2 was oxidized (GSSG 2 mM for 2 h) and, upon buffer exchange, 1 μM biosensor was incubated with NADPH (250 μM), DTT (5 mM), reduced *E. coli* Trx (10 μM) in the absence or presence of DTT (5 mM) or left untreated (control) and fluorescence monitored as indicated above during 1 h.

The percentage of reduced rxmRuby2 was calculated using the following formula: reduced rxmRuby2 (%) = [(FA - FA_{ox})/(FA_{red} - FA_{ox})] *100, where FA: Fluorescence Absorption at 560 nm of rxmRuby2 under assay conditions, FA_{ox}: Fluorescence Absorption at 560 nm of fully oxidized rxmRuby2, FA_{red}: Fluorescence Absorption at 560 nm of fully reduced rxmRuby2.

2.5.2. pH titration

The influence of the pH on the fluorescence of fully reduced and oxidized rxmRuby2 was studied under conditions of constant ionic strength (I = 0.15 M) using different buffer systems [23]. pH titration of reduced and oxidized rxmRuby2 was carried out at 25 °C in a solution containing Tris 6.2 mM, ethanolamine 6.2 mM, acetic acid 12 mM, DTPA 100 μM, NaCl 138 μM, NaOH 5 mM, at an initial pH of 9. The pH of the medium was stepwise modified by the accumulative addition of 0.4 M HCl up to a final pH of 4. The protein was diluted in the buffer solution to a final concentration of 1 μM and after 5 min equilibration, fluorescence absorption at 560 nm was recorded in a spectrofluorimeter (Cary Eclipse). The pH of the solution was measured immediately after the reaction and at the same temperature of the experiment (25 °C). pHs below and above 4 and 9 could not be tested due to biosensor instability (denaturation and aggregation). The apparent pKa of the chromophore was obtained by fitting the data to the Boltzmann equation (sigmoidal plot). Multiple regression statistical analysis of the fitted data yielded r^2 values of 0.98 and 0.99 for the reduced and oxidized sample, respectively.

2.5.3. Redox potential

The redox midpoint potential of rxmRuby2 was determined from the equilibrium constant obtained upon incubation (4 h) of the reduced biosensor with different ratios of GSSG/GSH in an oxygen-depleted atmosphere. The glutathione reductase assay [24] was used to estimate and remove any trace of GSSG present in commercial GSH prior to redox titration.

Reduced rxmRuby2 was prepared as indicated in section ***2.5.1*** and diluted to a final concentration of 5 μM by adding it to each well of a 96-well black plate (GREINER Bio ONE) containing 100 mM potassium phosphate (pH 7.0), 1 mM EDTA (thoroughly purged with argon), and varying concentrations of oxidized (0–100 μM) and reduced glutathione (0–10 mM). A control sample included protein incubated in the presence of 1 mM DTT (fully reduced protein) or 10 mM GSSG (fully oxidized protein). After equilibration of the protein samples under an argon atmosphere for 4 h at 25 °C, the redox state of the protein was assessed by spectrofluorimetry (λex = 480–580, λem = 600 nm).

The equilibrium reaction for the oxidation of rxmRuby2 by GSSG is:

$$rxmRuby2_{red} + GSSG \leftrightarrow rxmRuby2_{ox} + 2\ GSH$$

and the corresponding equilibrium constant (K_{eq}) is given by Equation (1):

$$K_{eq} = [rxmRuby2_{ox}]\ [GSH]^2\ /\ [rxmRuby2_{red}]\ [GSSG] \quad (1)$$

The fractional amount of reduced rxmRuby2 (R) in the presence of varying ratios of GSH/GSSG can be measured from the fluorescence absorption (560 nm) or emission (600 nm) of the protein chromophore, and is calculated as follow:

$$R = (F - F_{ox})\ /\ (F_{red} - F_{ox}) \quad (2)$$

Where F is the fluorescence absorption/emission of rxmRuby2 determined at a particular GSH/GSSG ratio, F_{red} and F_{ox} is the fluorescence absorption/emission of fully reduced and fully oxidized, respectively, rxmRuby2.

Furthermore, R can be related to K_{eq} by the following equation:

$$R = ([GSH_f]^2/[GSSG_f]\ /\ (K_{eq} + [GSH_f]^2/[GSSG_f]) \quad (3)$$

where the subindex f indicates the concentration of each species at equilibrium and determined according to the initial amount (i) of the reactants and R:

$$[GSH_f] = [GSH_i] - R[rxmRuby2_i]$$

$$[GSSG_f] = [GSSG_i] - R[rxmRuby2_i]$$

By using the Nernst equation (Eq. (4)), the different $[GSH_f]^2/[GSSG_f]$ ratios were converted into their corresponding E°′:

$$E^{\circ\prime}_{[GSHf]2/[GSSGf]} = E^{\circ}_{GSH} - (RT/nF)\ x\ \ln K_{eq} \quad (4)$$

where E° is the standard potential of GSH ($E^{\circ}_{GSH} = -240$ mV, at pH 7 and 25 °C) [25], R is the gas constant ($8.315\ J\ K^{-1}\ mol^{-1}$), T is the absolute temperature (303.15 K), n is the number of transferred electrons (2), and F is the Faraday constant ($9.649 \times 10^4\ C\ mol^{-1}$).

Finally, the midpoint redox potential of rxmRuby2 at pH 7 and 25 °C ($E^{\circ\prime}_{rxmRuby2}$) was calculated from the R *vs.* GSH/GSSG E°′ plot fitted to a Boltzmann equation yielding an r^2 value of 0.98.

2.6. Mammalian cell cultures

HEK-293 (ATCC CRL-1573) and HeLa (ATCC CCL-2) cells were cultured in DMEM (Thermo Fisher Scientific) supplemented with 10% (v/v) FBS. Cells were routinely propagated in 25 or 75 cm^2 tissue culture flasks at 37 °C and 5% CO_2 in a humidified incubator until reaching approximately 70% confluence. For experiments performed with cell suspensions, the cell monolayer was trypsinized and the density adjusted as required. All experiments performed in this study were conducted with cells cultured for less than fifteen passages.

2.7. Transfection and selection of stable redox-reporter cell lines

HEK-293 and HeLa cells were transfected with one of each plasmid: pIRES-eGFP (Addgene), pIRES-DsRed2 (Addgene), pCDNA3.1/Clover-mRuby2 (WT, Addgene), pCDNA3.1/CloverC49T-mRuby2C118S/T148C/D200C (RXM, this work), pCDNA3.1/rxmRuby2 (rxmRuby2, this work) or pCDNA3.1/rxYFP (rxYFP) [26].

For the generation of the transgenic cell lines, 1×10^6 cells were seeded in a 25 cm^2 T-flask and transfected with 10 μg plasmids and Lipofectamine 2000 (Thermo Fisher Scientific) according to manufacturer instructions. The experiments with cell lines transiently expressing the biosensor were conducted within 24–48 h post-transfection.

For the generation of stable cell lines, 24 h post-transfection and onwards cells were grown in medium containing Geneticin 250 μg/mL (G418, Sigma) during 30 days. Resistant cells expressing the RXM biosensor were sorted using a BD FACSAria™ Fusion (BD Biosciences). The cell suspension was filtered by a 50 μm nylon mesh before sorting. For detection of Clover or mRuby2 fluorescence, the following pair of λex/λem (in nm) were used: 488/530 ± 15 or 561/610 ± 10, respectively. Sort decision was based on FSC *vs.* SSC dot plots, excluding

doublets and including Clover and mRuby2 double positive cells on Clover *vs*. mRuby2 fluorescence intensity dot plots (Fig. S1A, B). Double positive cells were enriched using the purity sort mode and further isolated applying the Single Cell Deposition mode to place one cell per well into a 96-well plate containing 100 µL/well of culture medium supplemented with 20% (v/v) FBS. The stable cell clones were then amplified in culture medium supplemented with 10% (v/v) FBS and G418, further characterized by flow cytometry and cryopreserved.

2.8. Flow cytometry assays

HEK-293 or HeLa cells in the exponential growth phase and expressing transiently or stably WT Clover-mRuby2, RXM Clover-mRuby2, rxmRuby2 or rxYFP were exposed to different redox stimuli and fluorescence intensity (FI) was monitored over time. Non-treated samples were included as a control. HEK-293 and HeLa cells transfected with the pIRES-eGFP or pIRES-DsRed2 were used as flow cytometry compensation controls. At least three independent experiments were carried out for each determination.

Cells growing in 25 or 75 cm^2 T-flasks were trypsinized and resuspended in fresh culture medium before flow cytometry analysis with a BD FACSAria™ Fusion. For each sample, 10,000 counts gated on an FSC *vs*. SSC dot plot excluding cell doublets were recorded. The settings used for acquisition of fluorescence signal were λex/λem = 488/530 ± 15 for Clover, eGFP or rxYFP and λex/λem = 561/610 ± 10 for mRuby2, RXM, rxmRuby2 or DsRed2. For data acquisition, the BD FACSDIVA V8.0.1 software was used. The mean FI of Clover and mRuby2 double positive cells or mRuby2 or rxYFP single positive cells was analyzed using the FlowJo v.7.6.5 software (BD Biosciences). Quantitative assessment of the intracellular redox state of rxmRuby2 was achieved by normalizing its FI to Clover FI and by calibrating the measured signal to maximum and minimum FI values of both FP corresponding to conditions yielding fully reduced (5 mM DTT 60–120 min) and fully oxidized (100 µM diamide 30 min) redox biosensor, respectively.

2.9. Confocal microscopy

Cells in the exponential growth phase were seeded in sterile glass-bottom dishes (Thermo Fisher Scientific) and incubated for 24–48 h. Before analysis, the culture medium was replaced with fresh medium and the cells were challenged with none, diamide 100 µM and/or DTT 5 mM. Multiposition time-lapse imaging with a 20× oil immersion objective (NA 1.42) and z-stacks of 20–30 µm (step size of 1–1.5 µm) was performed at 37 °C and 5% CO_2 using an inverted confocal laser microscope (Leica TCS SP5). The signal for Clover and mRuby2 was detected using the following excitation and emission wavelengths: $\lambda_{ex}/\lambda_{em}$ 488/520 ± 10 nm and $\lambda_{ex}/\lambda_{em}$ 543/610 ± 20 nm, respectively. Images were acquired with the LAS AF Lite software (Leica Microsystems, Germany) and further analyzed with the ImageJ processing program.

2.10. Determination of reduced glutathione in protein-free cell extracts

The relative level of GSH in protein-free extracts of HEK-293 cells stably transfected with the RXM construct (clone E5) was determined using the fluorescent probe RealThiol [27]. Cells in exponential phase were harvested by trypsinization, resuspended in fresh culture medium to a density of 2 × 10^6 cells/mL and incubated for 2 h at 37 °C and 5% CO_2 to allow recovery from proteolytic stress. The cell suspensions were left untreated (control) or treated with diamide (100 µM), H_2O_2 (500 µM) or pyocyanin (500 µM) for 30 min. Ten minutes before stopping the treatments, 300 µL of the cell suspensions were separated for further analysis by flow cytometry in a BD FACSAria™ Fusion (for details on sample analysis see the previous section) and, in the remaining 600 µL, RT-AM ester (100 µM stock solution) was added at a final concentration of 5 µM and, in both cases, incubation extended for 10 min at room temperature. The RT-treated samples were washed twice with cold PBS to remove excess probe and lysed with 10% v/v ice cold trichloroacetic acid. The cell lysate was incubated on ice for 30 min and then centrifuged at 20,000 × *g* and 4 °C for 10 min to separate the supernatant. The cleared supernatant was analyzed in a spectrofluorimeter (Cary Eclipse) using λex/λem = 405/485 nm (detects GSH-bound probe) and λex/λem = 488/565 nm (detects free-probe). The results are expressed as the fluorescence ratio F405 (signal detected at λex/λem = 405/485 nm) *vs*. F488 (signal detected at λex/λem = 488/565 nm).

2.11. Statistical analysis

Statistic calculations were performed using the GraphPad Prism Software version 5.00 Demo (San Diego, CA, USA). Differences were considered statistically significant when $p < 0.05$ using ANOVA and Bonferroni's multiple comparison tests.

3. Results and discussion

3.1. In silico design and characterization of rxmRuby2

Structural alignments of red-shifted FPs (mCherry, PDB id: 2H5Q; Scarlet, PDB id: 5LK4; mRuby1, PDB id: 3U0L; mRuby2 and mRuby3) [28] against the redox sensible variants of GFP (roGFP2: PDB 1JC0) [11] and YFP (rxYFP: PDB 1H6R) [12] indicate that substituting Thr148 (β-strand 8) and Asp200 (β-strand 11) by cysteine would place two thiol groups at a suitable distance to reversibly create a disulfide bond. The *in silico* analysis further confirmed that oxidation/reduction would expose/protect the chromophore producing a change in fluorescence absorption and emission (Fig. 1A). Based on results obtained for rxYFP [29], we selected the FP showing the more favorable electrostatic environment for polarization of the thiol groups (i.e. reducing their pKa) and for the interaction with the redox substrate glutathione (net charge −2). As shown in Fig. 1B, mRuby and mRuby2 have the most positive environment in the neighborhood of the thiol moieties due to the vicinal Arg202 and Lys224 residues (Fig. 1A), which are absent in the other red-fluorescent proteins. On this basis and due to the higher brightness and photostability of mRuby2 [17], this protein was selected to construct a red-shifted redox sensor (hereafter named rxmRuby2). Although mRuby2 proved to be a monomeric protein under non-reducing conditions and in a wide range of concentrations [17,30], the solvent-exposed Cys118 was mutated to a serine in rxmRuby2 to avoid the potential formation of non-specific disulfides.

3.2. Biochemical characterization of rxmRuby2

Gel chromatography showed that oxidized recombinant rxmRuby2 eluted with a retention volume nearly corresponding to a monomeric protein species (apparent vs. theoretical molecular mass of 28.3 kDa *vs*. 27.4 kDa, respectively; Fig. 2A). At variance with GFP- and YFP-based redox biosensors, whose reduced and disulfide forms display different electrophoretic mobility on SDS-PAGE [12,14], both redox forms of rxmRuby2 display a similar migration pattern under denaturing conditions in a 15% (w/v) gel (Fig. 2A inset).

Under physiological pH 7.0, the fluorescence spectra of both reduced and oxidized rxmRuby2 (Fig. 2B) was essentially identical to that reported for the wild-type protein [17,28], with excitation and emission peaks at 560 and 600 nm, respectively, and a minor excitation shoulder around 520 nm. Apart from the change in amplitude in the excitation and emission peaks, no further alterations of the spectral properties of rxmRuby2 were observed upon oxidation. Thus, similar to rxYFP [12] and rxRFP [15,16], but in contrast to roGFP2 [31], the fluorescence of rxmRuby2 lacks a redox-dependent ratiometric behavior.

Treatment of reduced rxmRuby2 with an excess of different oxidants

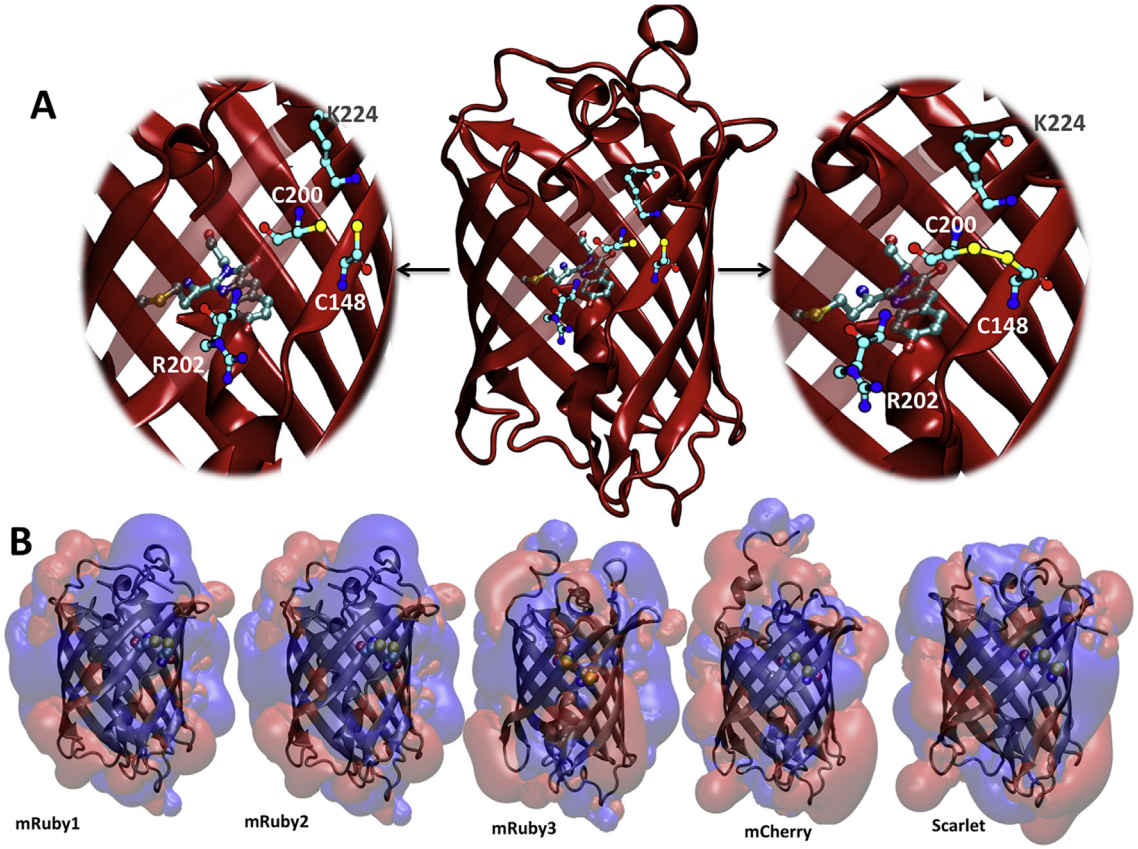

Fig. 1. 3D-model of rxmRuby2 and other red-fluorescent proteins. A) Cartoon representation of rxmRuby2 generated from the crystal structure of mRuby (Protein Data Bank code 3U0L). Residues discussed in the text are shown as balls and sticks in chalky colors, while the chromophore is shown in glossy representation. Insets on the reduced and oxidized states are shown at right and left sides, respectively. **B)** Isosurfaces of electrostatic potential represented on the backbone of different red-fluorescent proteins with a front-view at the reactive cysteine pair. Surfaces are drawn at +25 mV (blue) and −25 mV (red). The redox-active cysteine residues are shown for reference with space-filling representation. (For interpretation of the references to color in this figure legend, the reader is referred to the Web version of this article.)

(i.e. 50-fold for hydrogen peroxide, diamide, and GSSG, and 20-fold for ONOOH) led to a time-dependent decrease in the fluorescence of the protein (Fig. 2C). The magnitude and kinetics of the changes in fluorescence were also oxidant-dependent. GSSG and diamide shared a similar kinetic and level of decrease in rxmRuby2 fluorescence, while oxidation of the biosensor by H_2O_2 proved slower and significantly less effective. At 250 μM, peroxynitrite quenched almost irreversible rxmRuby2 fluorescence (not shown), likely due to direct damage of the chromophore. A potential overoxidation of rxmRuby2 cysteines by 250 μM H_2O_2 or 100 μM ONOOH was ruled out as full fluorescence was recovered upon treatment with DTT. In the presence of a stoichiometric concentration of human glutaredoxin (hGrx), GSSG reduced by 90% the relative fluorescence of rxmRuby2 within the first 2 min, and to almost null levels after 10 min. This shows that the redoxin catalyzes very efficiently the GSSG-dependent oxidation of rxmRuby2, as reported for related biosensors [32,33].

Independently of the nature of the oxidant, addition of an excess DTT (5 mM) to oxidized rxmRuby2 led to nearly full recovery (≥90%) in the fluorescence intensity of the biosensor within 46 min incubation (Fig. 2C). Nonetheless, the reduction kinetics was faster for the biosensor oxidized with GSSG (with or without Grx), diamide or ONOOH than with H_2O_2. This suggests that H_2O_2 generates oxidized forms of rxmRuby2 that are less efficiently reduced by DTT. In agreement with studies performed with related redox-sensitive FPs [6,12,13,32], hGrx (Fig. 2C) but not *E. coli* thioredoxin (Fig. 2D), even in a 10-fold excess with respect to rxmRuby2, accelerated the reduction of the disulfide form of the biosensor. Oxidized rxmRuby2 neither accepted reducing equivalents from NADPH (Fig. 2D). The catalytic control exerted by Grx on rxmRuby2 oxidoreduction suggests that real-time detection of changes in the GSH/GSSG ratio may be impaired in cells or intracellular compartments depleted or lacking the oxidoreductase.

A midpoint redox potential ($E^{\circ\prime}$) of −265 ± 22 mV was estimated for rxmRuby2 (Fig. 2E), which is almost identical to that reported for rxYFP (−261 mV) [12] and slightly less negative than that determined for roGFP2 (−272 mV [11]), and within the physiological range of the GSH redox potential (−240 mV to −320 mV) [9,10]. Worth noting, under our assay conditions (4 h incubation under semi anaerobic conditions and at pH 7.0) it was not possible to obtain 100% biosensor reduction for the highest GSH/GSSG ratio tested, likely due to the spontaneous oxidation of a minor fraction of GSH at physiological pH.

pH titration of fully reduced and fully oxidized biosensor revealed a chromophore' pK_a (defined as the pH value at which 50% of the maximal fluorescence is emitted) of 5.98 and 6.95, respectively (Fig. 2F). The pK_a of reduced rxmRuby2 is less acidic than that determined for mRuby (pK_a = 4.4) and mRuby2 (pK_a = 5.3), which suggests that the mutations altered the electrostatic environment of the chromophore favoring its deprotonation at a physiological pH range (see next section). In contrast, formation of the disulfide favors the protonation of the chromophore and a loss of fluorescence. Importantly, within the range of physiological pH (7.0–7.4) and independently of its redox state, rxmRuby2 exhibits a fluorescence intensity of ≥75% of its maximum.

3.3. Biological characterization of rxmRuby2-cell lines

The performance of rxmRuby2 was preliminary addressed in HEK-

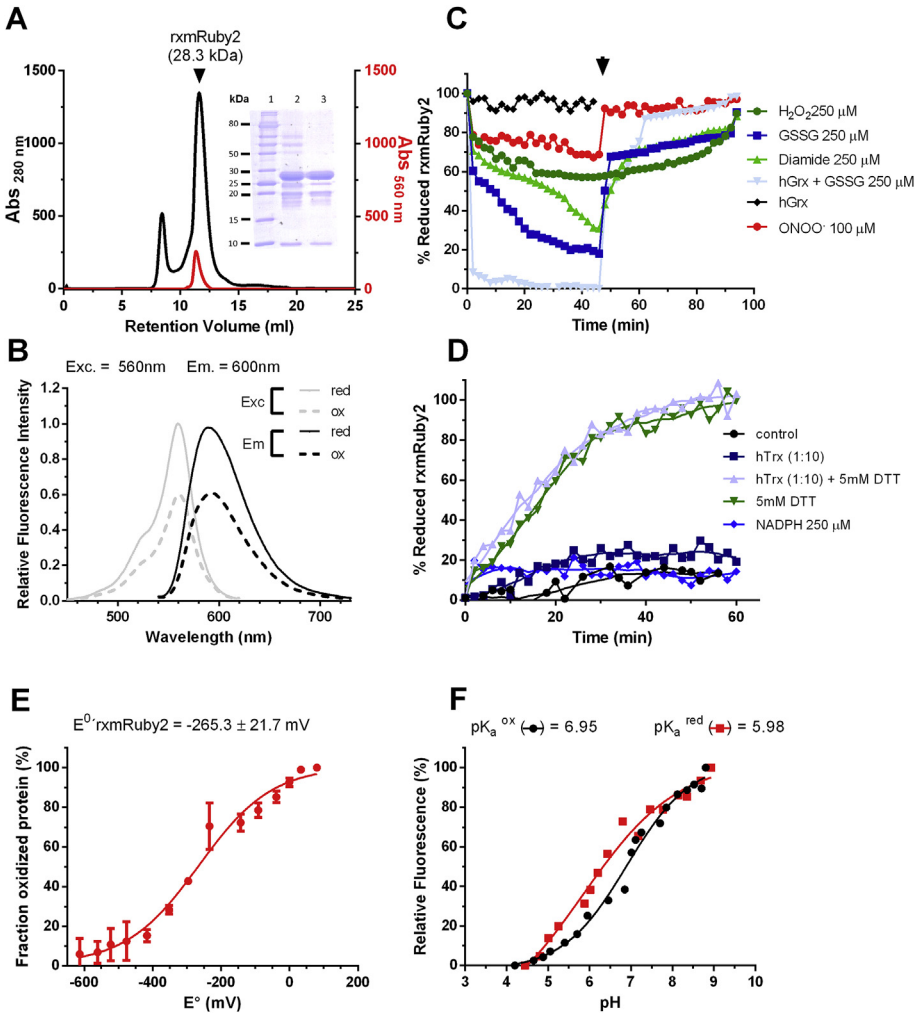

Fig. 2. Biochemical characterization of rxmRuby2. A) Gel filtration and SDS-PAGE analysis of rxmRuby2. Oxidized recombinant rxmRuby2 was separated by gel filtration chromatography (Superdex G75) and measuring absorbance at 280 nm (protein) and 560 nm (mRuby2 excitation fluorescence). The major protein peak containing oxidized monomeric rxmRuby2 and its apparent molecular mass is indicated with a head arrow and in kDa, respectively. Inset: SDS-PAGE (15% gel) of rxmRuby2 gel filtration peak run under non-reducing (lane 2) and reducing (10 mM DTT, lane 3) conditions. Lane 1 corresponds to the molecular weight marker. **B) Redox-dependent changes in the excitation and emission spectra of rxmRuby2.** Excitation (grey lines) and emission (black lines) spectra of fully reduced (solid lines) and oxidized (dashed lines) rxmRuby2. The wavelength corresponding to the excitation and emission peaks is indicated. **C) Time course oxidoreduction of rxmRuby2.** Reduced recombinant rxmRuby2 (5 µM) treated with 100 µM peroxynitrite (ONOOH, ●), or 250 µM H_2O_2 (●), diamide (▲), and GSSG in the absence (■) or presence of hGrx (5 µM; ▼) for 46 min. A sample of reduced rxmRuby2 (5 µM) containing oxidized hGrx (5 µM; ◆) was included as control. Thereafter, DTT (5 mM) is added to the samples and incubation extended for further 46 min. The arrow head indicates the time point at which DTT was added to the samples. **D) Time course reduction of rxmRuby2.** Disulfide form of recombinant rxmRuby2 (1 µM) non-treated with reductants (●) or treated for 60 min with NADPH (250 µM, ♦), DTT (5 mM, ▼), or reduced *E. coli* Trx (10 µM) in the absence (■) or presence of 5 mM DTT (▲). **E) The redox potential of rxmRuby2.** Redox titration of rxmRuby2 (5 µM) with varying [GSH]/[GSSG] ratios in PBS pH 7.0 at 25 °C. The fraction of oxidized protein was calculated as described in Material and Methods (section ***2.5.3***). The experimental standard redox potential of rxmRuby2 is shown inset. **F) pH-dependence of rxmRuby2 fluorescence**. Relative fluorescence of fully reduced (■) and oxidized (●) rxmRuby2 (1 µM) as a function of pH. The apparent pK_a of the chromophore for the reduced (pK_a^{red}) and the oxidized protein (pK_a^{ox}) is shown. For details on the experimental protocols see section ***2.5***.

293 and HeLa cells transiently expressing the redox biosensor (Fig. 3A–C and Fig. S1A). Upon trypsinization, the cells were immediately suspended in fresh medium, challenged with different redox stimuli and analyzed by flow cytometry (Fig. 3A). For both cell lines, rxmRuby2 fluorescence showed a time-dependent decrease in intensity during a 30 min treatment with 1 mM diamide that was fully reverted within the first 10 min after addition of 10 mM DTT (Fig. 3A). Interestingly, upon reductive stimulus, the relative signal of rxmRuby2 increased to values significantly higher than that recorded at the beginning of the assay and reached a plateau 30 min later. This result suggests that trypsinization perturbs the intracellular redox homeostasis and supports early observations that serine proteases induce ROS production in different human cell lines [34]. On the light of the results, all further experiments with cells in suspension were performed after rxmRuby2 signal spontaneously normalized (e.g. 60–120 min depending on cell type and trypsinization time).

In order to cancel-out non-redox phenomena that may alter the fluorescence signal of the reporter protein, rxmRuby2 was expressed fused to the Clover fluorescent protein (construct named RXM). Cells transfected with redox-insensitive Clover-mRuby2 were included as the control (WT) (Fig. 3B and C and Fig. S1B). Compared to the wild-type counterpart, the fluorescence intensity of rxmRuby2 was 6-fold lower in both cell lines (Table S1), which can be ascribed to the higher pK_a of the rxmRuby2 chromophore (Fig. 2F). Overall, the response of the redox biosensor fused to Clover was similar in both cell lines subjected to redox challenges while, as expected, wild-type mRuby2 and Clover signals were refractory to them (Fig. 3B and C). Briefly, a 30 min exposure to diamide (1 mM) induced a decrease in the relative fluorescence of rxmRuby2 that was fully reversible upon 35 min (HEK-293) or 50 min (HeLa) incubation with 10 mM DTT (Fig. 3B and C, respectively). Thus, Clover does not affect the response of rxmRuby2 and can be used as a normalization factor for quantitative assessments of cellular redox status.

Notably and independently of the biosensor configuration, the kinetic response of rxmRuby2 to the redox insults was cell-line dependent (Fig. 3A–C). For instance, rxmRuby2 oxidation and reduction was markedly faster in HEK-293 than in HeLa cells, with maximum differences observed 10 min after exposure to the oxidant and 30 min upon addition of the reducing agent. These results agree with a study showing that the distribution of oxidation equivalents on GSH and protein thiols (PSH) differs significantly between HEK-293 (GSH:PSH ratio = 44:56) and HeLa cells (GSH:PSH ratio = 33:67) upon diamide treatment (5 mM, 5 min) [35].

3.3.1. *Cells stably expressing the redox biosensor*

HEK-293 cells expressing stably Clover-rxmRuby2 or Clover-mRuby2 were enriched by cell sorting (Fig. 3D) and then subjected to redox stimuli (Fig. 3E). The redox-response of rxmRuby2 was similar to that observed for the pool of cells that expressed transiently the biosensor (Fig. 3B): diamide (1 mM) induced a rapid and sustained

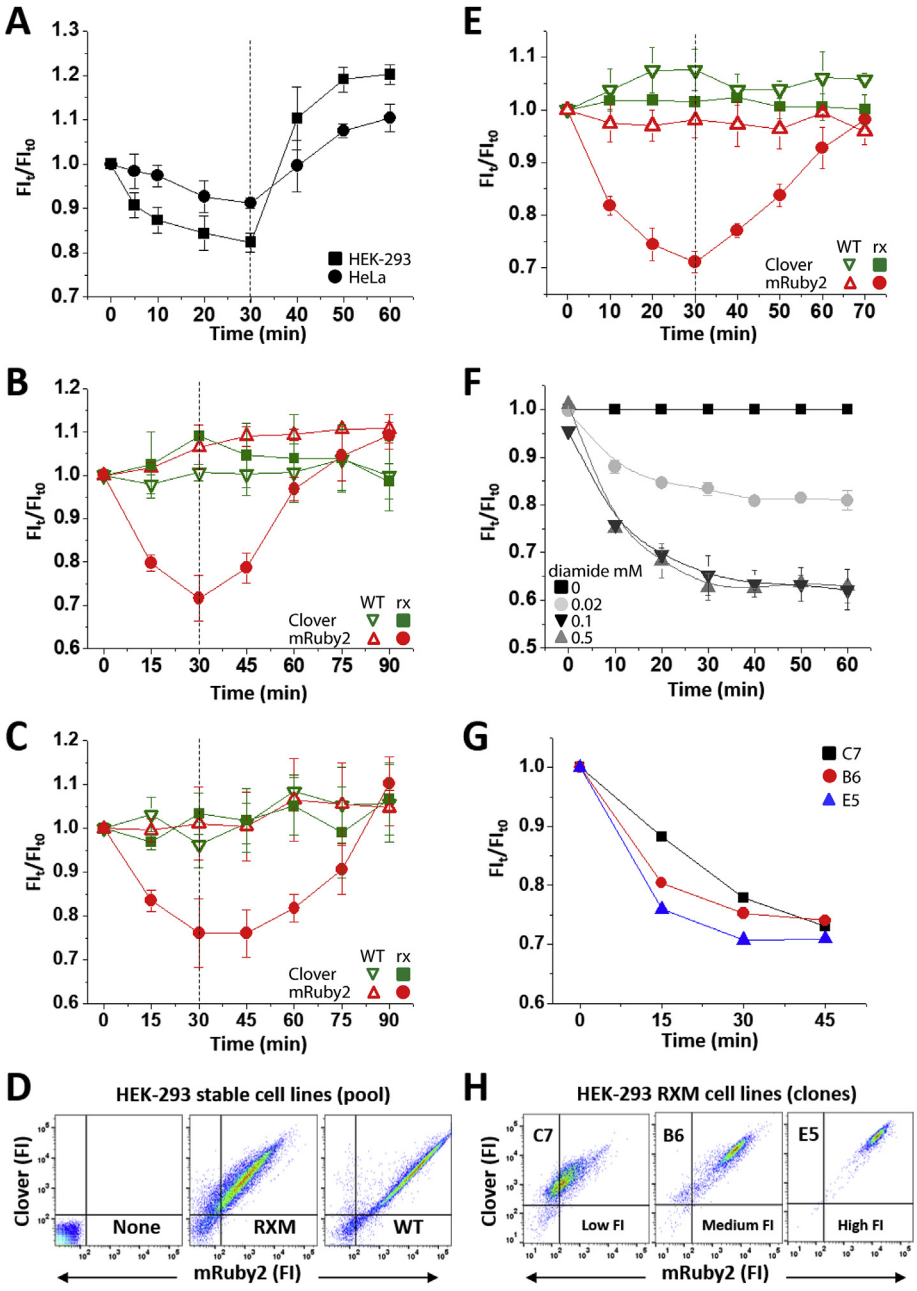

Fig. 3. Response of HEK-293 and HeLa cells expressing rxmRuby2, Clover/rxmRuby2 (RXM) or Clover/mRuby2 (WT) proteins to oxidative or reducing stimuli characterized by flow cytometry analysis. Time-course plots for the Fluorescence Intensity (FI) ratio of: **A)** cells transiently transfected with the rxmRuby2 vector, **B)** HEK-293 or **C)** HeLa cells transiently transfected with the Clover-rxmRuby2 vector (filled symbols) or Clover-mRuby2 vector (open symbols) and treated with 1 mM diamide at time point 0. **D)** Representative FI Clover *vs.* FI mRuby2 dot plots for HEK-293 stable cell lines expressing Clover-rxmRuby2 (RXM), Clover-mRuby2 (WT) or transfected with a mock vector. **E)** Time-course plots for the FI ratio corresponding to a double-positive (Clover-mRuby2 fluorescence) population of HEK-293 cells expressing stably Clover-rxmRuby2 (RXM, filled symbols) or Clover-mRuby2 (WT, open symbols) both treated with 1 mM diamide at time point 0. **F)** Time-course plots for the FI ratio of a population of HEK-293 cells expressing stably Clover-rxmRuby2 (RXM) and non-treated (■) or treated with different concentrations of diamide at time point 0. **G)** Time-course plot for the FI ratio from different clones (C7, B6 and E5) of HEK-293 cells that express stably the Clover-rxmRuby2 (RXM) treated with 1 mM diamide at time point 0 and **H)** the corresponding representative FI Clover vs. FI mRuby2 dot plots from each non-treated clone. Fluorescence intensity was determined for Clover (λex/λem 488/530 ± 15 nm) and/or mRuby2 (λex/λem 561/610 ± 10 nm). For each experiment, the FI at different time points (FIt) was normalized against FI at time 0 (FIt0). In **A**, **B**, **C**, and **E**, DTT 10 mM was added at time point 30 min (dashed line). The data are expressed as the mean ± standard deviation of at least three independent experiments, with the exception of (G) that is a representative experiment of two independent determinations.

decrease in rxmRuby2 signal that reached a minimum after 30 min whereas treatment with DTT (5 mM) recovered biosensor's fluorescence within the next 40 min (Fig. 3E). Furthermore, time-course and dose-response assays revealed that rxmRuby2 was sensitive enough to detect oxidative stress caused by 20 μM diamide, which corresponded to a 45% decrease in relative fluorescence signal 40 min after initiated the treatment (Fig. 3F).

Next, clones stably transfected with the RXM construct were isolated by the single-cell deposition technique according to the level of rxmRuby2 fluorescence intensity and subjected to oxidative challenge (Fig. 3 G–H). The oxidation kinetics of rxmRuby2 was proportional to the expression level of the biosensor (clone E5 > B6 > C7; Fig. 3G), indicating that cellular Grx and/or glutathione are not rate-limiting during the oxidation process and that the biosensor competes with endogenous PSH for its glutathione-dependent Grx-catalyzed oxidation. Despite the nearly 100-fold difference in rxmRuby2 expression between clone E5 and C7 (Fig. 3H), the decrease in FI displayed by these clones, measured at the shortest incubation time (15 min) upon addition of diamide, differed by only 2-folds (Fig. 3G). This highlights the sensitivity of rxmRuby2 to detect perturbations in the cytosolic GSH/GSSG ratio.

Supporting earlier observations made on the transiently transfected cells (section ***3.3.1***), the biosensor revealed that trypsin treatment led to a remarkable intracellular oxidation and that it took more than 2 h to the cells to restore their global PSH-redox balance (Fig. 4A). As observed in previous assays, the addition of 100 μM diamide 80 min after trypsinization (time-point at which the level of reduced rxmRuby2 is ~80%), produced a significant decrease in the fraction of reduced biosensor, which dropped to zero value about 50 min later. From this time-point (130 min) on, reduction of rxmRuby2 showed a sustained increase that approached 50% reduction for a 170 min time-window. The kinetics of rxmRuby2 oxidoreduction in the cytosol clearly differ between the oxidative and reductive phases, with the first presenting a higher rate than the second. A similar behavior was reported for rxYFP expressed in organelles with a more reducing millieu (nucleus, mitochondria, and cytosol) [36]. Worth noting, for all clones analyzed,

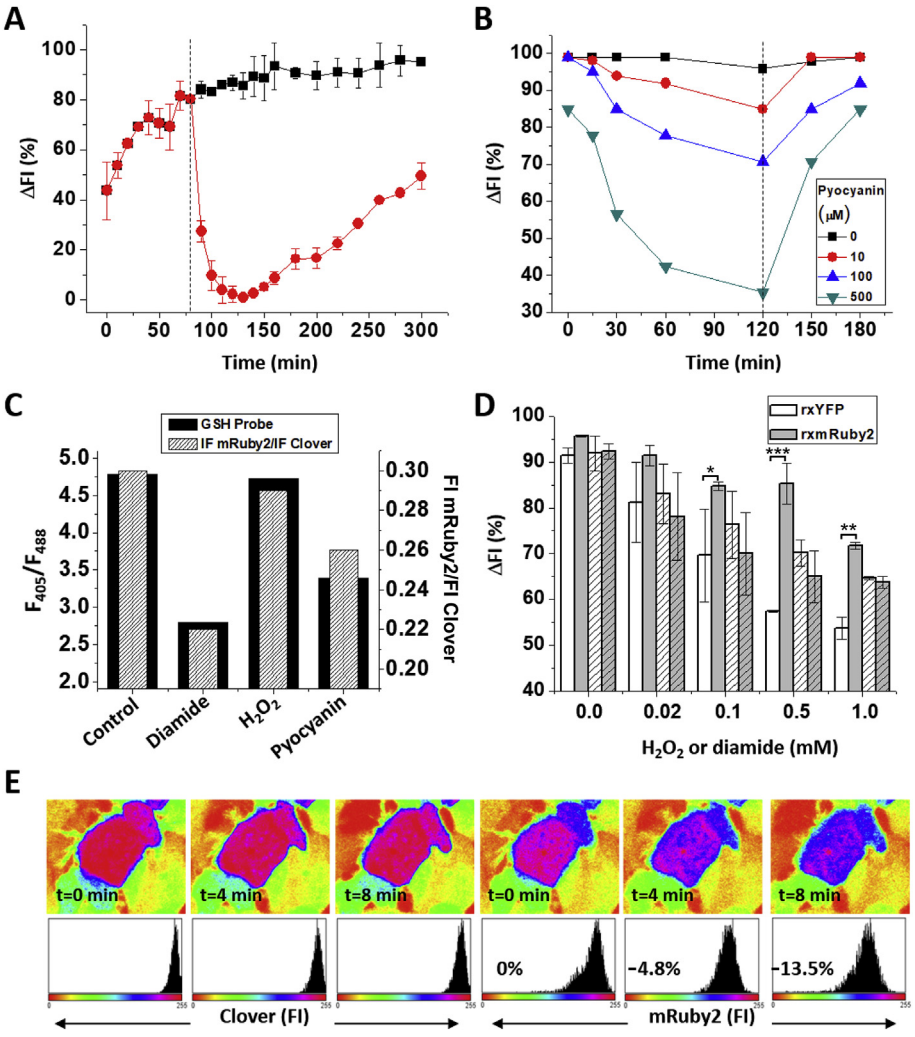

Fig. 4. Characterization of HEK-293 cells expressing Clover-rxmRuby2 by flow cytometry and confocal microscopy analysis. Time-course plots for the percentage variation (ΔFI %) of mRuby2 FI/Clover FI ratio in HEK-293 cells that stably express Clover-rxmRuby2 (RXM; clone E5) measured **A)** immediately after trypsinization and following incubation in the absence (■) or upon addition of 100 μM diamide (dashed-line; ●), **B)** after stimulation with different concentrations of pyocyanin added immediately at time point 0 and after addition of 10 mM DTT (dashed line). For each experiment, the ΔFI for fully reduced and oxidized biosensor was determined in cells treated for 60 min with 10 mM DTT and for 30 min with 100 μM diamide, respectively. **C)** Clone E5 was treated with none (control), diamide 100 μM, H_2O_2 500 μM, or Pyocyanin 500 μM. After 30 min, rxmRuby oxidation (expressed as the FI mRuby2/FI Clover ratio) was measured by flow cytometry and the relative level of free-glutathione (determined as the FI at 405/488 nm of the RT probe) was assessed in TCA-lysed cells by spectrofluorometry. **D)** HEK-293 cells expressing rxYFP (white bar) and transiently transfected with rxmRuby2 (grey bar) vector, exposed to different concentrations of H_2O_2 (plain bar) or diamide (striped bar) for 30 min. rxYFP and rxmRuby2 FI signals are expressed as ΔFI % normalized to the FI signal of the fully reduced form of each biosensor, which was achieved by incubating the cells with 5 mM DTT for 60 min. Statistical difference is expressed as *, $p < 0.05$, **, $p < 0.01$ and ***, $p < 0.001$. **E)** Time-lapse measurement by confocal microscopy of Clover (λex/λem 488/530 nm) and mRuby2 (λex/λem 543/600 nm) fluorescence of clone E5 upon treatment with 100 μM diamide. Images show the maximum intensity projection for z-stacks and the same pseudo-color scale was used to represent the fluorescence intensity of both reporter proteins. The inset values show the percentage decrease in rxmRuby2 signal normalized to Clover fluorescence. For **A** and **D**, the data correspond to the mean ± standard deviation of three independent experiments. **B** and **C** are representative experiments of at least two independent determinations. (For interpretation of the references to color in this figure legend, the reader is referred to the Web version of this article.)

expression of rxmRuby2 did not entail any growth phenotype and morphology defects, nor changes in sensitivity towards oxidants (not shown). Further studies were carried out with clone E5 because it displayed higher rxmRuby2 signal and response.

The capacity of rxmRuby2 to detect redox changes triggered by a more pathophysiological stimuli was tested using pyocyanin and H_2O_2. Pyocyanin is a potent redox cycling metabolite and virulence factor secreted by Pseudomonas during host colonization [37]. As shown in Fig. 4B, pyocyanin induced a dose- and time-dependent oxidation of rxmRuby2 that was reversible upon incubation with DTT (10 mM). rxmRuby2 was also capable to detect the time-dependent intracellular oxidative stress triggered by 100 μM H_2O_2 (Fig. S1C). Under identical assay conditions, 100 μM diamide produced a comparatively higher oxidation of the biosensor (Fig. S1C). This is not surprising and is in full agreement with our *in vitro* data (Fig. 2C) and with a previous report showing that at identical concentration of oxidants (500 μM), diamide induces a massive protein oxidation and rapid decrease in the GSH/GSSG ratio whereas H_2O_2 is a very selective protein oxidant that presents a slower kinetics for the reduction of the GSH/GSSG ratio in HEK-293 cells [38].

In order to provide compelling evidence about the selectivity of rxmRuby2 to detect changes in the GSH/GSSG pool, the level of intracellular free GSH was determined in cells expressing the redox biosensor and exposed to different oxidants (Fig. 4C). Free glutathione was measured using a highly specific chemical probe [27] and rxmRuby2 fluorescence was assessed in parallel by flow cytometry. As shown in Fig. 4C, the relative decrease in rxmRuby2 fluorescence exerted by diamide, H_2O_2 and pyocyanin was almost identical to the relative decrease in the content of free glutathione, thus, confirming the selectivity of the red-shifted biosensor in biological systems.

Next, rxmRuby2 was co-expressed transiently in HEK-293 cells stably transfected with rxYFP to compare *in situ* the sensitivity and specificity of our biosensor (Fig. 4D). Although both biosensors showed a similar dose-response to diamide, rxYFP proved more sensitive than rxmRuby2 to detect intracellular redox changes induced by the physiological oxidant H_2O_2. The difference in sensitivity was statistically significant ($p < 0.05$) at H_2O_2 concentrations ≥100 μM. Such selectivity is intriguing and cannot be ascribed to compartment- (pH) or cell-specific differences as both biosensors were co-expressed in the cytosol, neither to direct oxidation of rxYFP by H_2O_2 [36]. In contrast to diamide, which is a specific oxidant of thiols [39], μM concentrations of H_2O_2 proved very efficient in generating hydroxyl radicals through the Fenton reaction in HeLa cells [40]. It is then tempting to speculate that rxYFP is more sensitive than rxmRuby2 to become oxidized to its disulphide form upon reaction with H_2O_2 and/or that both proteins differ in their susceptibility toward overoxidation by H_2O_2 or radicals thereof.

Finally, we tested the suitability of Clover-rxmRuby2 for fluorescence microscopy-based assays. Time-lapse confocal microscopy performed in HEK-293 reporter cells treated with diamide (100 μM for 15 min) showed a sustained decrease in the rxmRuby2 signal that, for

the set of cells analyzed, reached a minimal value after 8 min (Fig. 4E), which corresponded to the fully oxidized form of the biosensor according to in-cell redox calibration of the biosensor (section ***2.8***). Again, the fluorescence of Clover displayed negligible changes during the course of the assay, which confirms its redox-silent nature and suitability as a normalizing factor.

3.4. Caveats for the use of rxmRuby2

The redox potential and substrate-specificity of rxmRuby2 make this biosensor suitable to detect small changes in the GSH/GSSG ratio in subcellular compartments with high GSH concentration and a predominantly reducing milieu. As shown here, Grx accelerates the equilibration of rxmRuby2 redox state with that of GSH/GSSG. Thus, reliable kinetics measurement require expressing the biosensor in cells and/or subcellular compartments containing Grx. Eventually, Grx can be fused to rxmRuby2 to provide a cell-independent kinetic control of biosensor oxide reduction but overexpression of the oxidoreductase should be avoided to maintain unaltered the intracellular redox homeostasis.

The pH sensitivity displayed by rxmRuby2 (pK_a of oxidized and reduced chromophore is 7 and 6, respectively) limits its use to organelles with pHs ≥ 7.0 (i.e. cytosol, nucleus, mitochondrial matrix), which warrants maximum fluorescence intensity (≥75%) of the biosensor.

Because the chromophore of rxmRuby2 lacks ratiometric spectra, quantitative determinations require *in situ* calibration of the biosensor (i.e. signal of fully reduced and oxidized rxmRuby2). The membrane permeant thiol reducing and oxidizing agents DTT and diamide, respectively, can be used for in-cell calibration of the biosensor as well as to verify the redox basis of the changes in fluorescence reported by rxmRuby2. Although this limitation may, to some extent, hamper the use of rxmRuby2 for deep-tissue or whole animal analysis, the recent development of Clover versions showing a redox-sensitive ratiometric behavior [41] offers strategies for engineering a ratiometric rxmRuby2.

Finally, though the spectra of rxmRuby2 presents a large Stokes shift (λex/λem = 560/600 nm), as for any other FPs, narrow band pass filters should be used to minimize excitation leakiness.

4. Conclusions

A novel red-shifted redox biosensor (rxmRuby2) has been rationally engineered and validated for quantitative measurements of redox states. rxmRuby2 showed selectivity for GSH/GSSG and Grx contributed to accelerating the thiol-disulfide equilibration of the probe with this pair. rxmRuby2 proved reliable in reporting the dynamics of intracellular redox changes in different cell types that express transiently or stably the biosensor. Despite the fluorescence of rxmRuby2 was 6-fold lower than that of the parental FP, its capacity to report redox changes was overall unaltered over a wide range of intracellular concentrations. Worth noting, fusion to a redox-insensitive fluorescent protein (Clover) allowed to cancel out cell-to-cell differences in expression levels, pH and/or other biophysical factors that may affect the fluorescence of these structurally related proteins. The red-shifted fluorescence of rxmRuby2 is compatible with the simultaneous use of multiple fluorophores or fluorescent proteins that present non-overlapping spectra, as shown here by co-expression of another redox biosensor (rxYFP) or a chemical fluorescent probe (RT). The molecular configuration of Clover-rxmRuby2 is also fully compatible with the fusion of Grx to its C-terminus, which should result in improved equilibration kinetics (from min/hour to sec/msec) with GSH/GSSG. Nonetheless, rxmRuby2 alone can be used as a model protein substrate to investigate the dynamics of thiol-disulfide exchange catalyzed by endogenous Grx in different subcellular compartments.

Thus, rxmRuby2 can be rated as a useful bio tool for high content analysis assays based on flow cytometry or confocal microscopy. Because red-shifted light penetrates deeper into tissues and provides lower levels of autofluorescence, rxmRuby2 appears as an appealing biosensor to address fundamental questions of redox biology based on deep-tissue and *in vivo* imaging.

Conflicts of interest

The authors declare that there are no conflicts of interest.

Acknowledgements

Dr. G. Pani (Institute of Physics, Catholic University Medical School, Rome, Italy) and Dr. J. Wang (Baylor College of Medicine, Houston, USA) are acknowledged for providing the pCDNA3.1/rxYFP vector and the RealThiol (RT) probe, respectively. This project was funded by ANII (FMV_1_2014_1_104000 and PR_FMV_2009_1_2617) and FOCEM (MERCOSUR Structural Convergence Fund), COF 03/11. CVP received financial support from Institut Pasteur de Montevideo Postdoctoral Programme, FS received a doctoral fellowship (POS_FMV_2015_1_1005325) and FK received a Master fellowship from ANII. CVP, SP, MC, and MB belong to the Uruguayan National System of Researchers (SNI).

Appendix A. Supplementary data

Supplementary data to this article can be found online at https://doi.org/10.1016/j.freeradbiomed.2019.01.035.

References

[1] E.M. Hanschmann, J.R. Godoy, C. Berndt, C. Hudemann, C.H. Lillig, Thioredoxins, glutaredoxins, and peroxiredoxins – molecular mechanisms and health significance: from cofactors to antioxidants to redox signaling, Antioxidants Redox Signal. 19 (2013) 1539–1605.
[2] A. Holmgren, C. Johansson, C. Berndt, M.E. Lönn, C. Hudemann, C.H. Lillig, Thiol redox control via thioredoxin and glutaredoxin systems, Biochem. Soc. Trans. 33 (2005) 1375–1377.
[3] C. Berndt, C.H. Lillig, A. Holmgren, Thioredoxins and glutaredoxins as facilitators of protein folding, Biochim. Biophys. Acta 1783 (2008) 641–650.
[4] Y.M. Go, D.P. Jones, Redox compartmentalization in eukaryotic cells, Biochim. Biophys. Acta 1780 (2008) 1273–1290.
[5] Y.S. Nkabyo, T.R. Ziegler, L.H. Gu, W.H. Watson, D.P. Jones, Glutathione and thioredoxin redox during differentiation in human colon epithelial (Caco-2) cells, Am. J. Physiol. Gastrointest. Liver Physiol. 283 (2002) G1352–G1359.
[6] H. Østergaard, C. Tachibana, J.R. Winther, Monitoring disulfide bond formation in the eukaryotic cytosol, J. Cell Biol. 166 (2004) 337–345.
[7] O. Björnberg, H. Østergaard, J.R. Winther, Measuring intracellular redox conditions using GFP-based sensors, Antioxidants Redox Signal. 8 (2006) 354–361.
[8] M.A. Comini, Measurement and meaning of cellular thiol:disulfide redox status, Free Radic. Res. 50 (2016) 246–271.
[9] A.J. Meyer, T.P. Dick, Fluorescent protein-based redox probes, Antioxidants Redox Signal. 13 (2010) 621–650.
[10] M. Schwarzländer, T.P. Dick, A.J. Meyer, B. Morgan, Dissecting redox biology using fluorescent protein sensors, Antioxidants Redox Signal. 24 (2016) 680–712.
[11] G.T. Hanson, R. Aggeler, D. Oglesbee, M. Cannon, R.A. Capaldi, R.Y. Tsien, S.J. Remington, Investigating mitochondrial redox potential with redox-sensitive green fluorescent protein indicators, J. Biol. Chem. 279 (2004) 13044–13053.
[12] H. Østergaard, A. Henriksen, F.G. Hansen, J.R. Winther, Shedding light on disulfide bond formation: engineering a redox switch in green fluorescent protein, EMBO J. 20 (2001) 5853–5862.
[13] M. Gutscher, A.L. Pauleau, L. Marty, T. Brach, G.H. Wabnitz, Y. Samstag, et al., Real-time imaging of the intracellular glutathione redox potential, Nat. Methods 5 (2008) 553–559.
[14] K. Kojer, M. Bien, H. Gangel, B. Morgan, T.P. Dick, J. Riemer, Glutathione redox potential in the mitochondrial intermembrane space is linked to the cytosol and impacts the Mia40 redox state, EMBO J. 31 (2012) 3169–3182.
[15] Y. Fan, Z. Chen, H.W. Ai, Monitoring redox dynamics in living cells with a redox-sensitive red fluorescent protein, Anal. Chem. 87 (2015) 2802–2810.
[16] Y. Fan, H.W. Ai, Development of redox-sensitive red fluorescent proteins for imaging redox dynamics in cellular compartments, Anal. Bioanal. Chem. 408 (2016) 2901–2911.
[17] A.J. Lam, F. St-Pierre, Y. Gong, J.D. Marshall, P.J. Cranfill, M.A. Baird, M.R. McKeown, J. Wiedenmann, M.W. Davidson, M.J. Schnitzer, R.Y. Tsien, M.Z. Lin, Improving FRET dynamic range with bright green and red fluorescent proteins, Nat. Methods 9 (2012) 1005–1012.
[18] R.B. Russell, G.J. Barton, Multiple protein sequence alignment from tertiary

structure comparison, Proteins Struct. Funct. Genet. 14 (1992) 309–323.
[19] W. Humphrey, A. Dalke, K. Schulten, VMD: visual molecular dynamics, J. Mol. Graph. Model. 14 (1996) 33–38.
[20] N. Eswar, B. Webb, M.A. Marti-Renom, M.S. Madhusudhan, D. Eramian, M.Y. Shen, U. Pieper, A. Sali, Comparative protein structure modeling using MODELLER, Curr. Protoc. Bioinformatics 15 (1) (2006) 5.6.1–5.6.30.
[21] S. Unni, Y. Huang, R.M. Hanson, M. Tobias, S. Krishnan, W.W. Li, J.E. Nielsen, N.A. Baker, Web servers and services for electrostatics calculations with APBS and PDB2PQR, J. Comput. Chem. 32 (2011) 1488–1491.
[22] L. Darré, M.R. Machado, A.F. Brandner, S. Ferreira, H.C. Gonzalez, S. Pantano, SIRAH: a structurally unbiased coarse-grained force field for proteins with aqueous solvation and long-range electrostatics, J. Chem. Theor. Comput. 11 (2015) 723–739.
[23] F. Sardi, B. Manta, S. Portillo-Ledesma, B. Knoops, M.A. Comini MA, G. Ferrer-Sueta, Determination of acidity and nucleophilicity in thiols by reaction with monobromobimane and fluorescence detection, Anal. Biochem. 435 (2013) 74–82.
[24] I. Carlberg, B. Mannervik, Glutathione reductase, Methods Enzymol. 113 (1985) 484–490.
[25] J. Rost, S. Rapoport, Reduction-potential of glutathione, Nature 11 (1964) 185–201.
[26] G. Maulucci, V. Labate, M. Mele, E. Panieri, G. Arcovito, T. Galeotti, H. Østergaard, J.R. Winther, M. De Spirito, G. Pani, High-resolution imaging of redox signaling in live cells through an oxidation-sensitive yellow fluorescent protein, Sci. Signal. 1 (2008) pl3.
[27] X. Jiang, et al., Quantitative real-time imaging of glutathione, Nat. Commun. 8 (2017) 16087.
[28] B.T. Bajar, E.S. Wang, A.J. Lam, B.B. Kim, C.L. Jacobs, E.S. Howe, M.W. Davidson, M.Z. Lin, J. Chu, Improving brightness and photostability of green and red fluorescent proteins for live cell imaging and FRET reporting, Sci. Rep. 6 (2016) 20889.
[29] R.E. Hansen, H. Østergaard, J.R. Winther, Increasing the reactivity of an artificial dithiol-disulfide pair through modification of the electrostatic milieu, Biochemistry 44 (2005) 5899–5906.
[30] S. Kredel, F. Oswald, K. Nienhaus, K. Deuschle, C. Röcker, M. Wolff, et al., mRuby, a bright monomeric red fluorescent protein for labeling of subcellular structures, PLoS One 4 (2009) e4391.
[31] C.T. Dooley, T.M. Dore, G.T. Hanson, W.C. Jackson, S.J. Remington, R.Y. Tsien, Imaging dynamic redox changes in mammalian cells with green fluorescent protein indicators, J. Biol. Chem. 279 (2004) 22284–22293.
[32] O. Björnberg, H. Østergaard, J.R. Winther, Mechanistic insight provided by glutaredoxin within a fusion to redox sensitive yellow fluorescent protein, Biochemistry 45 (2006) 2362–2371.
[33] A. Müller, J.F. Schneider, A. Degrossoli, N. Lupilova, T.P. Dick, L.I. Leichert, Systematic in vitro assessment of responses of roGFP2-based probes to physiologically relevant oxidant species, Free Radic. Biol. Med. 106 (2017) 329–338.
[34] K. Aoshiba, K. Yasuda, S. Yasui, J. Tamaoki, A. Nagai, Serine proteases increase oxidative stress in lung cells, Am. J. Physiol. Lung Cell Mol. Physiol. 281 (2001) 556–564.
[35] R.E. Hansen, D. Roth, J.R. Winther, Quantifying the global cellular thiol-disulfide status, Proc. Natl. Acad. Sci. U.S.A. 106 (2009) 422–427.
[36] A. Banach-Latapy, T. He, M. Dardalhon, L. Vernis, R. Chanet, M.E. Huang, Redox-sensitive YFP sensors for monitoring dynamic compartment-specific glutathione redox state, Free Radic. Biol. Med. 65 (2013) 436–445.
[37] S. Hall, C. McDermott, S. Anoopkumar-Dukie, A.J. McFarland, A. Forbes, A.V. Perkins, A.K. Davey, R. Chess-Williams, M.J. Kiefel, D. Arora, G.D. Grant, Cellular effects of pyocyanin, a secreted virulence factor of Pseudomonas aeruginosa, Toxins 8 (2016) 236.
[38] J.L. Gilge, M. Fisher, Y.-C. Chai, The effect of oxidant and the non-Oxidant alteration of cellular thiol concentration on the formation of protein mixed-disulfides in HEK 293 cells, PLoS One 3 (2008) e4015.
[39] N.S. Kosower, E.M. Kosower, Diamide: an oxidant probe for thiols, Methods Enzymol. 251 (1995) 123–133.
[40] J. Nakamura, E.R. Purvis, J.A. Swenberg, Micromolar concentrations of hydrogen peroxide induce oxidative DNA lesions more efficiently than millimolar concentrations in mammalian cells, Nucleic Acids Res. 31 (2003) 1790–1795.
[41] B.C. Campbell, G.A. Petsko, C.F. Liu, Crystal structure of green fluorescent protein clover and design of clover-based redox sensors, Structure 26 (2018) 225–237.